

Exploring Tensor Network Algorithms as a Quantum-Inspired Method for Quantum Reservoir Computing

Payal D. Solanki* and Anh Pham†

Deloitte Consulting LLP

(Dated: March 10, 2025)

Quantum reservoir computing (QRC) has emerged as a promising hybrid quantum machine learning (QML) method that leverages the complex dynamics of quantum systems and classical machine learning models. Motivated by the development of this new QML method, we explore how quantum-inspired techniques like tensor networks (TNs), specifically the Time Dependent Variational Principle (TDVP) with Matrix Product State (MPS), can be used for the QRC algorithm. To demonstrate the utility of our quantum-inspired method, we performed numerical experiments on the MNIST dataset and compared the performance of our quantum-inspired QRC with different classical machine learning (ML) methods. The results reveal that high-quality embeddings can be generated by performing the time-evolution of MPS system consisting of one-dimensional chain of Rydberg atoms. This quantum-inspired method is highly scalable, enabling the simulation of 100 qubits with a low classical computing overhead. Finally, this study also underscores the potential of tensor networks as quantum-inspired algorithms to enhance the capability of quantum machine learning algorithms to study datasets with large numbers of features.

I. INTRODUCTION

The convergence of quantum computing and machine learning has ushered in a new era of computational possibilities, collectively known as quantum machine learning (QML) [1–5]. This interdisciplinary field seeks to exploit the unique capabilities of quantum computers to enhance the performance of many machine learning tasks, potentially addressing problems that are intractable within the context of the classical computing paradigm. Among the various QML approaches, quantum reservoir computing (QRC) [6–10] has emerged as a particularly promising framework. By harnessing the complex dynamics of quantum systems, QRC offers an innovative method to process information and perform machine learning tasks, thereby circumventing some of the limitations inherent in traditional QML algorithms.

Inspired by classical reservoir computing (RC) [11–14], QRC leverages the intrinsic dynamics of quantum systems to process data. In classical RC, a fixed dynamical system, known as the reservoir, transforms input data into a high-dimensional space, thus enhancing the features used for training through simple linear regression. QRC extends this concept into the quantum realm, utilizing the exponentially large Hilbert space of quantum systems to generate correlations that are classically intractable.

The promise of many QML algorithms lies in the ability to use near-term quantum devices to produce correlations that would otherwise require exponential classical resources to simulate [1]. However, practical applications of QML are still limited, primarily due to the challenges posed by noisy intermediate-scale quantum de-

vices (NISQ) [15] and the complexity of training quantum models on quantum hardware. Additionally, the availability of quantum computers capable of handling a large number of qubits necessary to encode extensive data features is limited, further hindering the widespread adoption of QML [16, 17]. An alternative approach is to leverage quantum-inspired algorithms based on tensor network (TN) methods [18–22]. Specifically, tensor network algorithms can simulate the dynamics of certain quantum systems by representing the quantum states and operators in compressed form [23–25]. This approach significantly reduces the computational resources required, making it feasible to simulate specific quantum systems with a large number of qubits on classical hardware. Due to their utility, TN models have been effectively used as quantum-inspired algorithm to simulate certain quantum circuit models and QML techniques, enabling the exploration of many quantum algorithms using current classical devices [26–29].

Recent experimental study of the QRC algorithm has shown that this QML method can be implemented effectively on analog quantum hardware up to 108 qubits by encoding classical data to a 1D chain or 2D systems of Rydberg atoms [6]. These results have motivated our exploration of the tensor network algorithm as a quantum-inspired technique for QRC. Specifically, TNs can efficiently simulate quantum state evolutions [23, 30–33] and compute expectation values [19, 25] for certain quantum systems within a certain approximation of their dynamics [34, 35]. Secondly, tensor networks scale favorably with an increasing number of qubits for systems with low entanglement, mitigating the exponential complexity by exploiting quantum correlations, thus allowing the simulation of large-scale quantum systems with reduced computational overhead [18]. Finally, since the goal of the QRC technique is to generate new features based on the computation of expectation values from certain Hamiltonian dynamics [6], it naturally raises the question if

* paysolanki@deloitte.com

† anhdpham@deloitte.com

quantum-inspired technique like TNs with MPS can also produce similar ML performance. Such an investigation can provide a practical solution to explore QRC on classical hardware at scale, enabling researchers to investigate QRC properties and performance for datasets with more features, thereby accelerating algorithm development and providing insights into scalability and real-world applicability.

In this paper, we leveraged tensor network algorithms, specifically the time-dependent variational principle (TDVP) [31–33] and the matrix product state (MPS) to perform the time-evolution of 1D Rydberg atoms, with the goal of providing heuristic examples of how the QRC technique can be implemented at scale using a quantum-inspired technique. MPS-TDVP techniques based on the Lie-Trotter decomposition have been known to achieve a balance between performance and accuracy when they are used to simulate quantum dynamics such as time evolution [33]. To demonstrate the efficacy of TN, we performed numerical experiments using the MNIST [36] dataset using our MPS-based QRC for classification. Our numerical results suggest that the TDVP and MPS techniques are highly scalable, which opens up more possibilities to apply QRC to datasets with more features using classical computational resources.

II. METHODOLOGY

A. QRC Method with Rydberg Hamiltonian

The QRC algorithm consists of three primary components: data encoding into a Hamiltonian representing certain quantum dynamics, obtaining a quantum embedding through expectation value calculation, and a simple classical machine learning task. The QRC begins by encoding the data features into the parameters of the Rydberg Hamiltonian [38], as described in:

$$H = \sum_j \left[\frac{\Omega_j}{2} (e^{i\phi_j} |g_j\rangle \langle r_j| + e^{-i\phi_j} |r_j\rangle \langle g_j|) \right] - \sum_j \Delta_j \hat{n}^j + \sum_{j < k} V_{jk} \hat{n}^j \hat{n}^k \quad (1)$$

In this Hamiltonian, Ω_j represents the Rabi drive amplitude between a ground state ($|g_j\rangle$, with j indexing the atoms) and a highly excited Rydberg state ($|r_j\rangle$). Δ_j , the detuning of the driving laser field for atom j , and ϕ_j , the laser phase for atom j . Furthermore, V_{jk} describes the van der Waals interaction between atoms j and k , which can be derived from the geometry of the lattice as $V_{jk} = C/\|\mathbf{r}_j - \mathbf{r}_k\|^6$. Within our numerical experiments, we used a one-dimensional chain as the lattice geometry with the distance between two atoms being $11\ \mu\text{m}$ and the values of $\Omega = 2\pi$ and $\phi = 0$. The distance in the range of $10 - 11\ \mu\text{m}$ yields the best accuracy results for

the ML tasks. Other studies in QRC have also suggested distance within this value range for optimal ML performance [6].

To express the Hamiltonian in terms of Pauli matrices, we can use the following substitutions: $|g_j\rangle\langle r_j|$ is replaced by $\sigma_j^- = (\sigma_j^X - i\sigma_j^Y)/2$, which is the lowering operator; $|r_j\rangle\langle g_j|$ is replaced by $\sigma_j^+ = (\sigma_j^X + i\sigma_j^Y)/2$, which is the raising operator; and $\hat{n}^j = |r_j\rangle\langle r_j|$ is replaced by $(1 + \sigma_j^Z)/2$, which is the number operator. Using these substitutions, the Hamiltonian can be written as:

$$H = \sum_j \left[\frac{\Omega_j}{2} (\cos \phi_j \sigma_j^X - \sin \phi_j \sigma_j^Y) \right] - \sum_j \frac{\Delta_j}{2} (1 + \sigma_j^Z) + \sum_{j < k} \frac{V_{jk}}{4} (1 + \sigma_j^Z + \sigma_k^Z + \sigma_j^Z \sigma_k^Z) \quad (2)$$

Data encoding is achieved through site-dependent local detunings, represented as $\Delta_j = x_j$ [6]. Consequently, a N -qubit system is capable of encoding N features. Following data encoding, the final step involves classical post-processing. To achieve this, we obtain the data embedding vectors, which can be derived from the Hamiltonian dynamics of the quantum system. Specifically, after encoding the data through site-dependent local detunings, represented as $\Delta_j = x_j$, the N -qubit system transitions from an all spin-up ground state under the influence of the specifically designed Rydberg Hamiltonian. The quantum dynamics are then examined over several successive time steps. At each time step, the expectation values of local observables are measured, typically one- and two-point correlators on a computational basis, such as $\langle Z_j \rangle$ and $\langle Z_j Z_k \rangle$. These local observables then form the data embedding vectors, $u_i[n]$, with i indexing the different correlators and probe times. These vectors are essential for the classical post-processing step. To obtain these expectation values, the TN algorithm has been used.

B. Tensor Network Methods for Dynamical Simulation of Rydberg Hamiltonian for QRC

In the realm of tensor network algorithms, the time-dependent variational principle (TDVP) is a robust method to simulate the dynamics of quantum systems, particularly those with a substantial number of qubits. TDVP can be implemented in two primary forms: single-site TDVP and two-site TDVP. Both approaches are crucial for efficiently evolving quantum states represented by Matrix Product States (MPS) under the influence of a Hamiltonian, represented by the Matrix Product Operator (MPO) format. Single-site TDVP focuses on updating one site (or tensor) of the MPS at a time, ensuring relatively low computational cost and suitability for large systems, while maintaining unitary time evolution, energy conservation [32], and numerical stability

[44, 45]. However, single-site TDVP uses a fixed-rank integration scheme, which does not allow the bond dimension to grow during the time evolution, thus limiting its applications to simulate only certain quantum dynamics [35, 46]. In contrast, TDVP for two sites updates pairs of neighboring sites simultaneously, allowing for a more accurate representation of correlations, especially in systems interacting strongly, but has a much higher computational cost [31].

For the simulation of the quantum system in this study, the TeNPy library [39] was utilized. TeNPy is a versatile and efficient library for implementing tensor network algorithms, including single-site and two-site TDVP. It provides robust tools for handling MPS and MPO representations, making it ideal for simulating quantum system evolution. In this simulation, we encoded the classical data in a 1D chain. The Rydberg Hamiltonian was represented using the MPO format, and the quantum system, initially set in an all-up state, was evolved using the TDVP algorithm. Correlators were computed at each time step to generate the nonlinear embedding.

It is important to note that the interaction term V_{jk} decreases very rapidly as the distance between the atoms increases. Consequently, V_{jk} becomes negligible for the farthest neighbors, which can be safely ignored in the calculations. This rapid decrease in interaction strength allows us to reduce the dimensions of MPOs, leading to a significant reduction in computational time. Furthermore, we can optimize data embedding by excluding expectation values $\langle Z_j Z_k \rangle$ for pairs of sites j and k that do not interact in the Hamiltonian. By focusing only on the relevant interactions, we can streamline our data processing and further enhance computational efficiency. For instance, if we consider the case of 25 qubits, the original number of correlators for a particular time step would be 325. However, by choosing a truncation limit for V_{ij} of 10^{-4} , the number of correlators can be reduced to 247.

C. Data Preprocessing, QRC Simulation, and Classical Machine Learning Methods

To investigate the efficacy of our quantum-inspired QRC technique, we applied the method to perform a classification task using the MNIST dataset [36]. The initial step in our methodology involves preprocessing the MNIST dataset, which consists of 60,000 training samples and 10,000 test samples, each represented as grayscale images of 28×28 pixels. Principal Component Analysis (PCA) [40] was used to reduce the dimensionality of the data to facilitate the embedding process. Each component of the PCA-reduced data was mapped to a qubit as described in the methodology.

The embeddings were generated by computing the expectation values of the local observables at each time step. The parameters of the Rydberg Hamiltonian include a chain geometry with a scale of $11 \mu\text{m}$, the Rabi

frequency Ω set to 2π . The simulation was run with a time step of $0.5 \mu\text{s}$ up to a total time of $4 \mu\text{s}$.

Once the quantum embeddings were obtained, we performed classification using a simple linear fitting model with the quantum embeddings as input. In addition, we also compared the performance of our quantum-inspired QRC model with a linear and nonlinear ML models using the original PCA-reduced data as input. All of our ML classification tasks were performed using the keras package [41]. The models and their parameters are described below:

- **Linear fitting of the original data:** A simple linear model was trained on the PCA-reduced data, consisting of a single dense layer with 10 units and L1 regularization. The optimizer used was Adam, and the loss function was Sparse Categorical Cross Entropy.
- **Non-linear fitting of the original data:** A 4-layer feedforward neural network (NN) model with two hidden layers and L1 regularization was trained on the PCA-reduced data. The architecture includes two dense layers with 100 units each

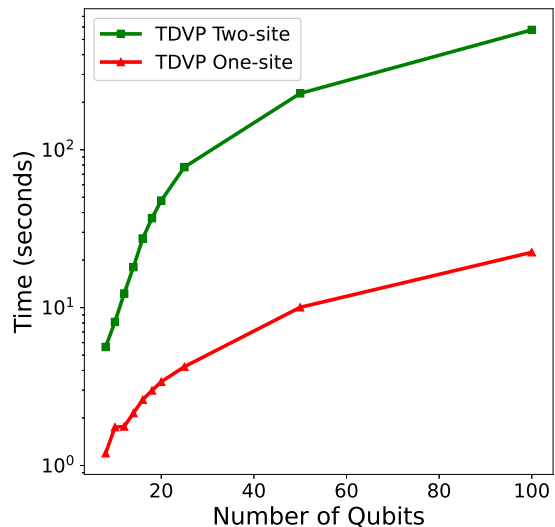


FIG. 1. **Scaling analysis of different simulation methods to calculate the quantum embeddings in the QRC method.** Specifically, time complexity (in seconds) was taken for data embedding computation using the TDVP-two site, and TDVP-one site with increasing number of qubits on a normal laptop (AMD Ryzen 7 PRO 7730U with Radeon Graphics, 16.0 GB RAM). The experiments were conducted using the parameters $\Omega = 2\pi$ and $\phi = 0$. The ground state, where all qubits are in the “up” state, was evolved using the Rydberg Hamiltonian up to $T = 4 \mu\text{s}$ with time steps of $0.5 \mu\text{s}$. For TDVP two-site, we have chosen the maximum bond dimension to be 100, and the bond dimension was fixed during the time evolution using the one-site TDVP. The y-axis is presented in logarithmic scale.

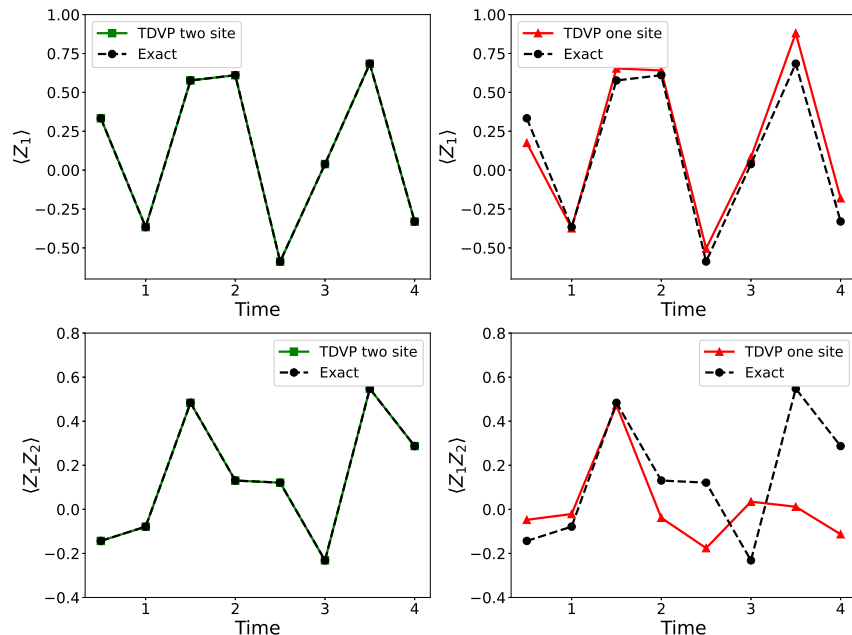


FIG. 2. **Accuracy of different TN methods in calculating the time-evolution dynamics of 1D chain of Rydberg atoms.** Here we give an example of computing the expectation values associated with the dynamics of the first and second qubit. The one-body $\langle Z_1 \rangle$ and the two-body $\langle Z_1 Z_2 \rangle$ expectation values at different time steps were calculated using the TDVP two-site, and TDVP one-site. The results were compared against exact diagonalization. The maximum bond dimension was set at 100 for the TDVP two-site. The experiments were conducted using 8 qubits, and the parameters of the Rydberg Hamiltonian are: $\Omega = 2.2\pi$, $\Delta = 2.4\pi$, and $\phi = 0$.

(ReLU activation) and a dense output layer with 10 units (softmax activation). The optimizer used was Adam, and the loss function was Sparse Categorical Crossentropy.

- **Linear fitting of quantum embeddings:** A linear model with L1 regularization was trained on the quantum embeddings. The model consisted of a single dense layer with 10 units and an L1 regularizer. The optimizer used was Adam, and the loss function was Sparse Categorical Cross Entropy.

The accuracy of the models was determined by comparing the predicted labels with the true labels of the test set, enabling a direct comparison of the performance between the quantum embeddings and the PCA embeddings.

III. RESULTS AND DISCUSSIONS

A. Scaling Analysis of Quantum Inspired QRC Method

In this section, we present a time complexity analysis to calculate the QRC embedding of a single data point in the MNIST dataset using two different methods to simulate Rydberg Hamiltonian dynamics: the TDVP-two site, and the TDVP-one site. Note that for TDVP two-site,

we have chosen the maximum bond dimension to be 100.

Figure 1 illustrates the time taken for data embedding computation across various qubit values using two different methods: TDVP-two site and TDVP-one site. The tensor network algorithm shows a steady increase in computation time as the number of qubits increases. This shows scalability better than other methods like exact diagonalization. It should be noted that the tensor network algorithm does not exhibit the same exponential increase in computation time as observed with exact diagonalization. This suggests that the tensor network approach scales more favorably with the number of qubits, making it a more viable option for practical applications involving larger quantum systems.

Among the TDVP methods, the one-site TDVP method is the most efficient and scalable method for generating data embedding with increasing qubit numbers. However, it is important to note that tensor network simulations may not accurately simulate quantum dynamics like time evolution for a high number of qubits since the bond dimensions were kept fixed during the time evolution within the one-site TDVP algorithm. Nevertheless, the embeddings generated by the one-site TDVP method still enable accurate ML performance, which will be discussed further in the next section.

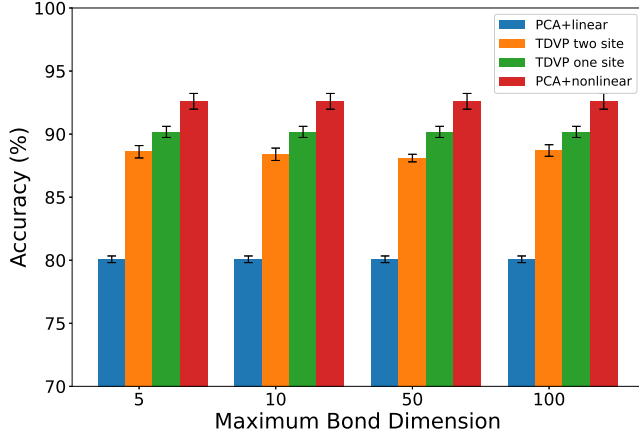


FIG. 3. **Quantum inspired QRC performance for 12 qubits (12 features) with varying bond dimensions for 1D chain of Rydberg atoms.** Here the quantum embeddings were generated with the two-site TDVP method at different bond lengths. This result was compared against the quantum embedding generated by the TDVP one site method. For this study, we also compared the quantum-inspired results against results from classical models (linear and NN) with classical features.

B. Quantum Inspired QRC Model Performance

To evaluate the performance of our method, we investigated the accuracy of computing the correlators using different time evolution methods, the impact of the bond dimensions on model performance, and a comprehensive comparison with various classical and quantum-inspired models using the MNIST dataset in our numerical experiments. Our findings reveal intriguing insights into the efficacy of these methods in improving machine learning tasks. To begin with, we examined the accuracy of the correlators obtained using different methods. Specifically, we considered the one-body correlator $\langle Z_1 \rangle$ and the two-body correlator $\langle Z_1 Z_2 \rangle$ versus evolution time. Although the correlators derived from the tensor network algorithms may not be exact, their temporal trends closely resemble the exact results. This observation is illustrated in Fig.(2), where we compare the correlators (for an 8-qubit system) of data embeddings using the exact diagonalization method versus the TDVP one-site, and TDVP two-site methods. The TDVP two-site method, in particular, achieves a high degree of accuracy. It is important to note that for the purposes of QRC, the exact accuracy of the correlator values is not critical; the embeddings can still yield the appropriate model accuracy.

To further validate the utility of tensor network algorithms, we investigated the impact of varying bond dimensions on model accuracy using the TDVP two-site method. As shown in Fig. 3, the performance of different classical models with classical features represents

the upper and lower bounds for our quantum-inspired algorithm with different bond dimensions. Our findings indicate that the bond dimension does not have a significant impact on the accuracy of the QRC. The accuracy achieved with the QRC closely matches the accuracy of the non-linear model and outperform a classical linear model demonstrating the effectiveness of the tensor network approach. Overall, this implies that quantum-inspired method like the one-site TDVP can generate adequate quantum embeddings. Despite the one-site TDVP not producing the most accurate correlators, it remains a viable option due to its efficiency and the minimal impact of bond dimension on accuracy.

Subsequently, we investigate the performance of our quantum-inspired QRC model with an increasing number of features using the one-site TDVP technique. Specifically, we compare the accuracy of three models as discussed in Section IIC: linear fitting of original data (PCA+linear), neural network model with original data (PCA+nonlinear), and linear model with quantum embeddings generated by the one-site TDVP method in the QRC algorithm. The model accuracy is illustrated in Fig.(4). It should be noted that the plot includes error bars, representing the results of experiments conducted using k-fold cross-validation with $k = 5$. The analysis of Fig.(4) reveals several key insights into the performance of quantum embeddings compared to PCA embeddings. In particular, the QRC method consistently outperforms the linear model with classical features. As the number of qubits increases, the accuracy of the model also increases and then saturates. This result is expected since more features allow for a richer representation of information in the data. Importantly, the accuracy corresponding to QRC embedding using the TDVP one-site method matches that of the nonlinear model with classical features within the error range. This highlights the main advantage of the QRC approach, demonstrating that it can achieve comparable performance to more complex nonlinear models while utilizing a linear framework. The error bars are relatively small, suggesting that the results are consistent and reliable. Consequently, this demonstrates that the use of tensor network algorithms, such as the one-site TDVP method, can be useful as a quantum-inspired QRC method for datasets with a large number of features.

IV. CONCLUSION AND OUTLOOK

This paper explored Quantum Reservoir Computing using Tensor Network algorithms to enhance the performance of classical machine learning tasks as a quantum-inspired method. By encoding data features into a Rydberg Hamiltonian and evolving the quantum system, we extracted high-quality embeddings using different TN techniques to simulate the time-evolution dynamics. In addition, this quantum-inspired algorithm was shown to be efficient enough to generate good

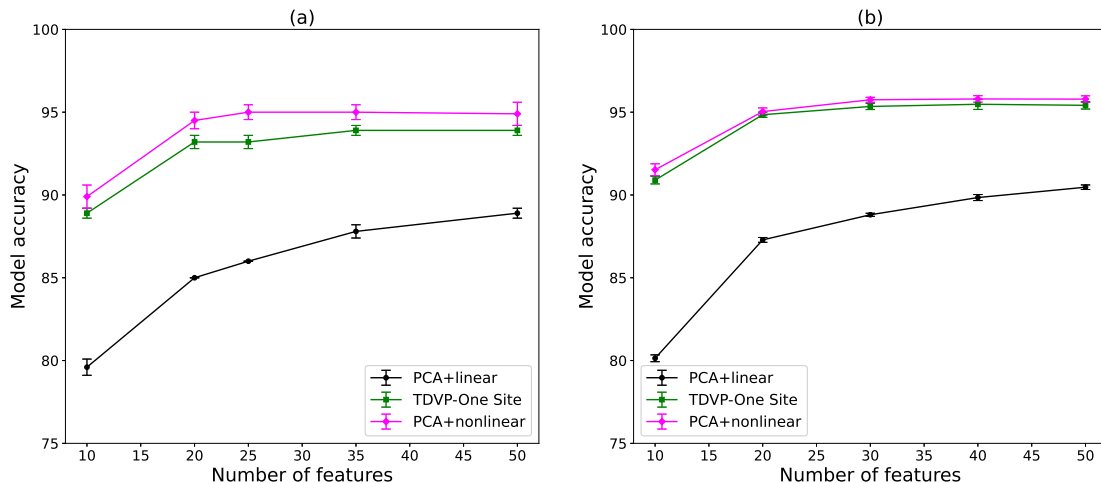


FIG. 4. **Model accuracy comparison between the quantum-inspired QRC methods, and classical ML algorithms.** a) This graph was generated using 10000 train set and 1000 test set points. b) This graph was generated using whole dataset and k fold cross validation using $k = 5$.

quantum embeddings for a large number of qubits in our numerical experiments, which enhance the overall performance of classical ML models. A future extension of this quantum-inspired algorithm could consider combining TDVP techniques at one and two sites to balance precision and performance [47], increasing its applicability for different datasets. Finally, we hope that the results of this study will motivate further studies on the possible limits of using TN to study quantum dynamics and other QML applications. Specifically, in the case of QRC, since we have only explored the utility of this quantum-inspired method in the MNIST dataset, a further exploration would be to identify other datasets where the exact simulation of quantum dynamics is critical for ML performance due to the rapid increase in entanglement of quantum phases during the time evolution process [42, 43].

Acknowledgements We would like to thank Milan Koprnjača, Sheng-Tao Wang, and Scott Buchholz for their feedback and discussion.

Disclaimer About Deloitte: Deloitte refers to one or more of Deloitte Touche Tohmatsu Limited (“DTTL”), its global network of member firms, and their related entities (collectively, the “Deloitte organization”). DTTL (also referred to as “Deloitte Global”) and each of its member firms and related entities are legally separate and independent entities, which cannot obligate or bind

each other in respect of third parties. DTTL and each DTTL member firm and related entity is liable only for its own acts and omissions, and not those of each other. DTTL does not provide services to clients. Please see www.deloitte.com/about to learn more.

Deloitte is a leading global provider of audit and assurance, consulting, financial advisory, risk advisory, tax and related services. Our global network of member firms and related entities in more than 150 countries and territories (collectively, the “Deloitte organization”) serves four out of five Fortune Global 500® companies. Learn how Deloitte’s approximately 460,000 people make an impact that matters at www.deloitte.com. This communication contains general information only, and none of Deloitte Touche Tohmatsu Limited (“DTTL”), its global network of member firms or their related entities (collectively, the “Deloitte organization”) is, by means of this communication, rendering professional advice or services. Before making any decision or taking any action that may affect your finances or your business, you should consult a qualified professional adviser. No representations, warranties or undertakings (express or implied) are given as to the accuracy or completeness of the information in this communication, and none of DTTL, its member firms, related entities, employees or agents shall be liable or responsible for any loss or damage whatsoever arising directly or indirectly in connection with any person relying on this communication. Copyright © 2025 Deloitte Development LLC. All rights reserved..

[1] J. Biamonte, P. Wittek, N. Pancotti, P. Rebentrost, N. Wiebe, and S. Lloyd, *Quantum machine learning*, Na-

ture **549**, 195 (2017).

- [2] H.-Y. Huang, R. Kueng, and J. Preskill, Information-theoretic bounds on quantum advantage in machine learning, *Physical Review Letters* **126**, 190505 (2021).
- [3] Y. Liu, S. Arunachalam, and K. Temme, A rigorous and robust quantum speed-up in supervised machine learning, *Nature Physics* **17**, 1013 (2021).
- [4] E. R. Anschuetz, H.-Y. Hu, J.-L. Huang, and X. Gao, Interpretable quantum advantage in neural sequence learning, *PRX Quantum* **4**, 020338 (2023).
- [5] H.-Y. Huang, M. Broughton, M. Mohseni, R. Babbush, S. Boixo, H. Neven, and J. R. McClean, Power of data in quantum machine learning, *Nature communications* **12**, 2631 (2021).
- [6] M. Kornjača, H.-Y. Hu, C. Zhao, J. Wurtz, P. Weinberg, M. Hamdan, A. Zhdanov, S. H. Cantu, H. Zhou, R. A. Bravo, *et al.*, Large-scale quantum reservoir learning with an analog quantum computer, arXiv preprint arXiv:2407.02553 <https://doi.org/10.48550/arXiv.2407.02553> (2024).
- [7] J. García-Beni, G. L. Giorgi, M. C. Soriano, and R. Zambrini, Scalable photonic platform for real-time quantum reservoir computing, *Physical Review Applied* **20**, 014051 (2023).
- [8] L. Govia, G. Ribeill, G. Rowlands, H. Krovi, and T. Ohki, Quantum reservoir computing with a single nonlinear oscillator, *Physical Review Research* **3**, 013077 (2021).
- [9] R. Martínez-Peña, J. Nokkala, G. L. Giorgi, R. Zambrini, and M. C. Soriano, Information processing capacity of spin-based quantum reservoir computing systems, *Cognitive Computation*, 1 (2023).
- [10] P. Mujal, R. Martínez-Peña, J. Nokkala, J. García-Beni, G. L. Giorgi, M. C. Soriano, and R. Zambrini, Opportunities in quantum reservoir computing and extreme learning machines, *Advanced Quantum Technologies* **4**, 2100027 (2021).
- [11] G. Tanaka, T. Yamane, J. B. Héroux, R. Nakane, N. Kanazawa, S. Takeda, H. Numata, D. Nakano, and A. Hirose, Recent advances in physical reservoir computing: A review, *Neural Networks* **115**, 100 (2019).
- [12] B. Schrauwen, D. Verstraeten, and J. Van Campenhout, An overview of reservoir computing: theory, applications and implementations, in *Proceedings of the 15th european symposium on artificial neural networks. p. 471-482 2007* (2007) pp. 471–482.
- [13] K. Nakajima and I. Fischer, *Reservoir computing* (Springer, 2021).
- [14] M. Lukoševičius and H. Jaeger, Reservoir computing approaches to recurrent neural network training, *Computer science review* **3**, 127 (2009).
- [15] K. Bharti, A. Cervera-Lierta, T. H. Kyaw, T. Haug, S. Alperin-Lea, A. Anand, M. Degroote, H. Heimonen, J. S. Kottmann, T. Menke, *et al.*, Noisy intermediate-scale quantum algorithms, *Reviews of Modern Physics* **94**, 015004 (2022).
- [16] M. Cerezo, A. Arrasmith, R. Babbush, S. C. Benjamin, S. Endo, K. Fujii, J. R. McClean, K. Mitarai, X. Yuan, L. Cincio, *et al.*, Variational quantum algorithms, *Nature Reviews Physics* **3**, 625 (2021).
- [17] J. R. McClean, S. Boixo, V. N. Smelyanskiy, R. Babbush, and H. Neven, Barren plateaus in quantum neural network training landscapes, *Nature communications* **9**, 4812 (2018).
- [18] R. Orús, A practical introduction to tensor networks: Matrix product states and projected entangled pair states, *Annals of physics* **349**, 117 (2014).
- [19] U. Schollwöck, The density-matrix renormalization group in the age of matrix product states, *Annals of physics* **326**, 96 (2011).
- [20] U. Schollwöck, The density-matrix renormalization group, *Reviews of modern physics* **77**, 259 (2005).
- [21] S.-J. Ran, E. Tiritto, C. Peng, X. Chen, L. Tagliacozzo, G. Su, and M. Lewenstein, *Tensor network contractions: methods and applications to quantum many-body systems* (Springer Nature, 2020).
- [22] F. Verstraete, V. Murg, and J. I. Cirac, Matrix product states, projected entangled pair states, and variational renormalization group methods for quantum spin systems, *Advances in physics* **57**, 143 (2008).
- [23] G. Vidal, Efficient classical simulation of slightly entangled quantum computations, *Physical review letters* **91**, 147902 (2003).
- [24] S. R. White, Density matrix formulation for quantum renormalization groups, *Physical review letters* **69**, 2863 (1992).
- [25] K. Kechedzhi, S. Isakov, S. Mandrà, B. Villalonga, X. Mi, S. Boixo, and V. Smelyanskiy, Effective quantum volume, fidelity and computational cost of noisy quantum processing experiments, *Future Generation Computer Systems* **153**, 431–441 (2024).
- [26] S. Shin, Y. S. Teo, and H. Jeong, Dequantizing quantum machine learning models using tensor networks, *Physical Review Research* **6**, 023218 (2024).
- [27] J. Chen, F. Zhang, C. Huang, M. Newman, and Y. Shi, Classical simulation of intermediate-size quantum circuits, arXiv preprint arXiv:1805.01450 <https://doi.org/10.48550/arXiv.1805.01450> (2018).
- [28] E. Stoudenmire and X. Waintal, Opening the black box inside grover’s algorithm, *Physical Review X* **14**, 041029 (2024).
- [29] T. Begušić, J. Gray, and G. K.-L. Chan, Fast and converged classical simulations of evidence for the utility of quantum computing before fault tolerance, *Science Advances* **10**, eadk4321 (2024).
- [30] G. Vidal, Classical simulation of infinite-size quantum lattice systems in one spatial dimension, *Physical review letters* **98**, 070201 (2007).
- [31] J. Haegeman, C. Lubich, I. Oseledets, B. Vandereycken, and F. Verstraete, Unifying time evolution and optimization with matrix product states, *Physical Review B* **94**, 165116 (2016).
- [32] J. Haegeman, J. I. Cirac, T. J. Osborne, I. Pižorn, H. Verschelde, and F. Verstraete, Time-dependent variational principle for quantum lattices, *Physical review letters* **107**, 070601 (2011).
- [33] S. Paeckel, T. Köhler, A. Swoboda, S. R. Manmana, U. Schollwöck, and C. Hubig, Time-evolution methods for matrix-product states, *Annals of Physics* **411**, 167998 (2019).
- [34] T. Chanda, P. Sierant, and J. Zakrzewski, Time dynamics with matrix product states: Many-body localization transition of large systems revisited, *Phys. Rev. B* **101**, 035148 (2020).
- [35] B. Kloss, Y. B. Lev, and D. Reichman, Time-dependent variational principle in matrix-product state manifolds: Pitfalls and potential, *Phys. Rev. B* **97**, 024307 (2018).
- [36] L. Deng, The mnist database of handwritten digit images for machine learning research [best of the web], *IEEE signal processing magazine* **29**, 141 (2012).

- [37] B. A. Martin, T. Ayril, F. Jamet, M. J. Rančić, and P. Simon, Combining matrix product states and noisy quantum computers for quantum simulation (2024), arXiv:2305.19231 [quant-ph].
- [38] J. Wurtz, A. Bylinskii, B. Braverman, J. Amato-Grill, S. H. Cantu, F. Huber, A. Lukin, F. Liu, P. Weinberg, J. Long, *et al.*, Aquila: Quera’s 256-qubit neutral-atom quantum computer, arXiv preprint arXiv:2306.11727 <https://doi.org/10.48550/arXiv.2306.11727> (2023).
- [39] J. Hauschild and F. Pollmann, Efficient numerical simulations with tensor networks: Tensor network python (tenpy), SciPost Physics Lecture Notes , 005 (2018).
- [40] K. P. F.R.S., Liii. on lines and planes of closest fit to systems of points in space, The London, Edinburgh, and Dublin Philosophical Magazine and Journal of Science **2**, 559 (1901).
- [41] F. Chollet *et al.*, Keras, <https://keras.io> (2015).
- [42] N. Schuch, M. M. Wolf, K. G. H. Vollbrecht, and J. I. Cirac, On entropy growth and the hardness of simulating time evolution, New Journal of Physics **10**, 033032 (2008).
- [43] A. M. Läuchli and C. Kollath, Spreading of correlations and entanglement after a quench in the one-dimensional bose–hubbard model, Journal of Statistical Mechanics: Theory and Experiment **2008**, P05018 (2008).
- [44] C. Lubich, I. V. Oseledets, and B. Vandereycken, Time integration of tensor trains, SIAM Journal on Numerical Analysis **53**, 917–941 (2015).
- [45] E. Kieri, C. Lubich, and H. Walach, Discretized dynamical low-rank approximation in the presence of small singular values, SIAM Journal on Numerical Analysis **54**, 1020 (2016).
- [46] S. Goto and I. Danshita, Performance of the time-dependent variational principle for matrix product states in the long-time evolution of a pure state, Phys. Rev. B **99**, 054307 (2019).
- [47] J.-W. Li, A. Gleis, and J. von Delft, Time-dependent variational principle with controlled bond expansion for matrix product states, Phys. Rev. Lett. **133**, 026401 (2024).